Journal of Volcanology and Geothermal Research 408 (2020) 107097

Contents lists available at ScienceDirect

Journal of Volcanology and Geothermal Research

journal homepage: www.elsevier.com/locate/jvolgeores

Underwater records of submarine volcanic activity: El Hierro (Canary Islands 2011–2012) eruption

Maria Jose Jurado [a,*], Maurizio Ripepe [b], Carmen Lopez [c], Antonio Ricciardi [d], Maria Jose Blanco [e], Giorgio Lacanna [b]

[a] Geosciences Barcelona CSIC, Lluis Solé Sabaris s/n, Barcelona 08028, Spain
[b] Dipartimento di Scienze della Terra, Via La Pira, 4, Firenze 50121, Italy
[c] Observatorio Geofísico Central, Instituto Geográfico Nacional (IGN), C/Alfonso XII, 3, Madrid 28014, Spain
[d] Dipartimento Scienze della Terra, Sapienza Università di Roma, Roma 00185, Italy
[e] Centro Geofísico de Canarias, Instituto Geográfico Nacional (IGN), C/La Marina 22, Santa Cruz de Tenerife 38001, Spain

ARTICLE INFO

Article history:
Received 1 June 2020
Received in revised form 16 October 2020
Accepted 19 October 2020
Available online 24 October 2020

Keywords:
Monitoring
Submarine volcanic eruption
Geophone array

ABSTRACT

We present the monitoring of a submarine volcanic eruption that took place near the southernmost emerged land of El Hierro Island (Canary Islands, Spain), from October 2011 to February 2012. Right after the onset of the eruption, in mid-October 2011, we deployed an offshore geophone array for the purpose of monitoring the submarine eruptive activity signals. It acquired continuous data from October 2011 to May 2012, sometime after the end of the eruption. The array consisted of 8 high-frequency, 3-component geophones assembled into a cable string, with 6 m of separation. The geophone string was installed in La Restinga Harbor at a distance of less than 2 km from the volcanic edifice. The dataset acquired with the array is a unique continuous acoustic record of the activity associated with this eruption. We analyzed the continuous signal of the eruptive activity, with special interest in those events reflecting the eruption dynamics. Our results show that the geophone array was recording acoustic waves from a back-azimuth source corresponding to the position of the submarine vent, traveling at a speed of 1510 m/s, compatible with the speed of sound in water. Acoustic data shows a good correlation with the seismic data recorded on land for the case of earthquake occurrence. In addition, it provides relevant information towards the understanding of the eruptive surface activity. Therefore, this methodology can be successfully used in cases of submarine eruptions.

1. Introduction

More than 75% of the magmatic output on Earth occurs in underwater environments—mainly at mid-ocean ridges. However, in only a few cases, has submarine volcanic activity been documented by multibeam surveys or by recording visible manifestations on the sea surface. For example the birth of Surtsey volcanic islands in Iceland (Thorarinsson et al., 1964; Kokelaar and Durant, 1983) and the Serreta submarine eruption near Terceira Island in the Azores (Forjaz, 2000) The evolution of the most recent Nishinoshima volcano eruption in Japan was monitored by Kaneko et al. (2019) using satellite observations and by Shinohara et al. (2017) using ocean bottom seismometers (OBSs).

Submarine volcanoes occur worldwide but usually at water depths where the deployment of monitoring instrumentation to gather data on the volcanic activity can be extremely challenging. Therefore, a submarine eruption close to El Hierro island, occurring at relatively shallow depths (tens to few hundred meters), provided an excellent opportunity to test new techniques and methodologies and to improve the existing observational networks.

Only a few active volcanoes have been directly observed and monitored using hydroacoustic sensors: the West Mata submarine volcano in the North-East Lau Basin, South-West Pacific Ocean (Resing et al., 2011; Caplan-Auerbach et al., 2014) and the Monowai submarine volcano, Kermadec Arc (Chadwick et al., 2008a). Observations of shallow submarine activity have also been done at Kilauea and Mauna Loa by scuba divers and remotely operated vehicles (ROV). However, performing long-term monitoring in such an environment is challenging, and thus is normally done only for short periods of time and through the use of automatic ocean bottom systems (Hernández et al., 2014). NW Rota-1 and Axial eruptions were both recorded acoustically as well.

Nishida and Ichihara (2016) carried out a real-time infrasonic monitoring of the eruption at a remote volcanic island close to Nishinoshima island using seismoacoustic cross correlation; they monitored and applied this method to a pair of online stations on Chichijima. One was the horizontal ground velocity that was recorded at a permanent seismic station operated by the Japan Meteorological Agency (JMA). The

* Corresponding author.
E-mail address: mjjurado@ictja.csic.es (M.J. Jurado).

https://doi.org/10.1016/j.jvolgeores.2020.107097
0377-0273/

other was the air pressure recorded at the JMA Meteorological Observatory.

This and other studies have demonstrated that hydroacoustics has a high detection capacity with a great potential as a remote monitoring tool. This technique has also been recognized by the international Comprehensive Test Ban Treaty Organization (CTBTO), a pioneer in the use of hydrophone stations worldwide to monitor underwater nuclear testing (Fox et al., 2001).

Tepp et al. (2019) used the CTBTO hydrophone stations to monitor the 2-week-long Ahyi shallow submarine eruption, in the Northern Mariana Islands. Hydroacoustic eruption signals were observed by the regional Mariana seismic network and on distant hydrophones, and National Oceanic and Atmospheric Administration (NOAA) scuba divers working in the area soon after the onset of the eruption heard and felt underwater explosion sounds Tepp et al. (2019). Only yellow-orange bubble mats throughout the neighboring areas were observed but no other surface manifestations of the eruption were reported or observed in satellite data. Tepp et al. (2019) studied in detail the eruption chronology and its morphologic impacts by analyzing seismic and hydroacoustic recordings and through repeated bathymetric mapping. The eruption produced several thousand short, impulsive hydroacoustic signals—that were interpreted as underwater explosions—as well as tremors observed near the beginning and end of the sequence. The initial tremor, which occurred for 2 h, has been interpreted as small phreatomagmatic explosions. This tremor was followed by a 90-min pause before the characteristic impulsive signals began. Occasional tremors (lasting up to a few minutes) during the last 1.5 days of the eruption were interpreted as due to more sustained eruptive activity. Bathymetric changes show that a new crater, about 150 m deep, formed near the former summit, and a large landslide chute formed on the southeastern flank.

Another reference contribution was part of the HUGO project, and consisted in the installation of a single hydrophone at Lō'ihi volcano in Hawaii. Caplan-Auerbach and Duennebier (2001) proved that eruptive submarine activity was in fact recorded. They were also successful in discriminating the signals caused by submarine landslides, which occurred along its southern flank. Acoustic monitoring is also increasingly used by the World Meteorological Organization (WMO) and by the International Civil Aviation Organization (ICAO) as the appropriate monitoring tool to promptly detect volcanic eruptions worldwide. It has been shown that techniques based on small-aperture and low-cost infrasound arrays, can easily detect the location of acoustic sources produced by subaerial volcanic activity (Ripepe and Marchetti, 2002; Yamakawa et al., 2018).

Dziak et al. (2008) presented other examples of successful hydroacoustic monitoring of volcanic activity. In 2005, three Ocean Bottom Hydrophones (OBHs) were deployed for 7 months on the caldera floor of Brothers volcano, located within the southern Kermadec intraoceanic arc, located roughly 350 km northeast of New Zealand, where they recorded low-frequency (0.5–10 Hz) acoustic waves from regional and local earthquakes, as well as 2470 discrete harmonic tremor events, caused by volcanic activity.

Remote detection of hydroacoustic signals from submarine volcanic activity were also described by Sugioka et al. (2005). Submarine volcanic events often generate acoustic waves (T-waves) traveling over long distances through the low velocity channel (SOFAR) of the ocean. By a method of coherent stacking of T-waves from submarine volcanic activity in northern Mariana, the authors found a significant semidiurnal variation of T-wave travel times. They interpreted the large T-phase travel time variation as a consequence of the large up-and-down movement of seawater around the axis of the SOFAR channel. Acoustic measurements made at NW Rota-1 volcano in the Mariana Arc recorded sound between 1 and 60 Hz, during Strombolian explosions (Chadwick et al., 2008b). In August 2009, after years of low-intensity explosive activity, hydroacoustic instrumentation successfully recorded a major landslide event. This event was triggered by an unusually large-scale eruption, which produced an acoustic signal 10 times greater than the normal background level of the eruptive activity. It was the first documented sequence of a submarine volcano for an intrusion-eruption-landslide event (Chadwick et al., 2012). Also relevant to acoustic measurements are the studies by Dziak et al. (2015) and Schnur et al. (2017). The 2015 eruption of the Axial seamount was recorded both seismically and acoustically in real time (Wilcock et al., 2016; Caplan-Auerbach et al., 2017). Lyons et al. (2019) used low-frequency sound in the atmosphere (infrasound) to examine the source mechanics of shallow submarine explosions from Bogoslof volcano, Alaska. They showed that the infrasound originates from the oscillation and rupture of magmatic gas bubbles that initially form from submerged vents, but which grow and burst above sea level. They modeled the low-frequency signals as over-pressurized gas bubbles that grow near the water-air interface, which require bubble radii of 50–220 m, having been described for explosive subaqueous eruptions for more than a century. Lyons et al. (2019) presented a unique geophysical record of this phenomenon and proposed that the dominant role of seawater during the effusion of gas-rich magma into shallow water is to repeatedly produce a gas-tight seal near the vent. This resealing mechanism leads to sequences of violent explosions and the release of large, bubble-forming volumes of gas activity we describe as hydrovulcanian. Recently, Lyons et al. (2020) recorded infrasound from an explosive eruption occurring in shallow seawater, providing extensive insights into eruption dynamics in this unique environment. The dominance of low-frequency infrasound (0.1–1 Hz) is attributed to eruptions occurring beneath tens of meters of seawater. Higher-frequency infrasound signals were mostly limited to eruptions where the vent was isolated from major interaction with seawater or in several cases where a lava dome grew above sea level.

In this study, we present an innovative methodology and approach to detect and locate events generated at active volcanoes based on: 1) the deployment of a submarine geophone array, 2) comparison of the acoustic signal recorded by the geophone array with the on-land record of from seismic station, and 3) the spatial location of the submarine source of acoustic/seismic signals.

2. Geological setting

El Hierro is the smallest and youngest island of the group of seven volcanic islands that form the Canarian Archipelago located off the NW coast of Africa. The oldest subaerial rocks reported were dated at 1.12 Ma (Guillou et al., 1996). The island has an area of 273 km^2, rising from a base at 4000 m depth to an altitude of 1500 m above sea level at Mal Paso (Carracedo, 1994). More than 250 subaerial cones and submarine vents have been mapped, 31% of which are offshore in the rift zone (Becerril et al., 2013). Arcuate, horseshoe-shaped depressions are known to be associated with several giant gravitational landslides that characterize the flanks of the island: El Golfo in the northwestern sector, Las Playas in the southeast and El Julan in the southwest (Fig. 1A).

At the southernmost of El Hierro island, the IGN-CSIC deployed an array of geophones in La Restinga (Fig. 1B), on the seabed of the fishing harbor, endowed with eight sensors at variable depths ranging between 6 and 12 m below sea level (Fig. 1C).

The last 500 years is considered to be a period of quiescent volcanic activity in the region. However, in 1793 the population of Restinga felt intense seismic activity that could have been related to an intrusive magmatic episode that either did not end in eruption or culminated in an unregistered submarine eruption (Villasante-Marcos and Pavón-Carrasco, 2014), such as occurred in 2011–2012.

3. The 2011–2012 El Hierro eruption

Starting on July 10th, 2011seismic unrest signals observed by the IGN monitoring network installed on El Hierro island, indicated the beginning of a period of volcanic unrest that lasted for 83 days. After more

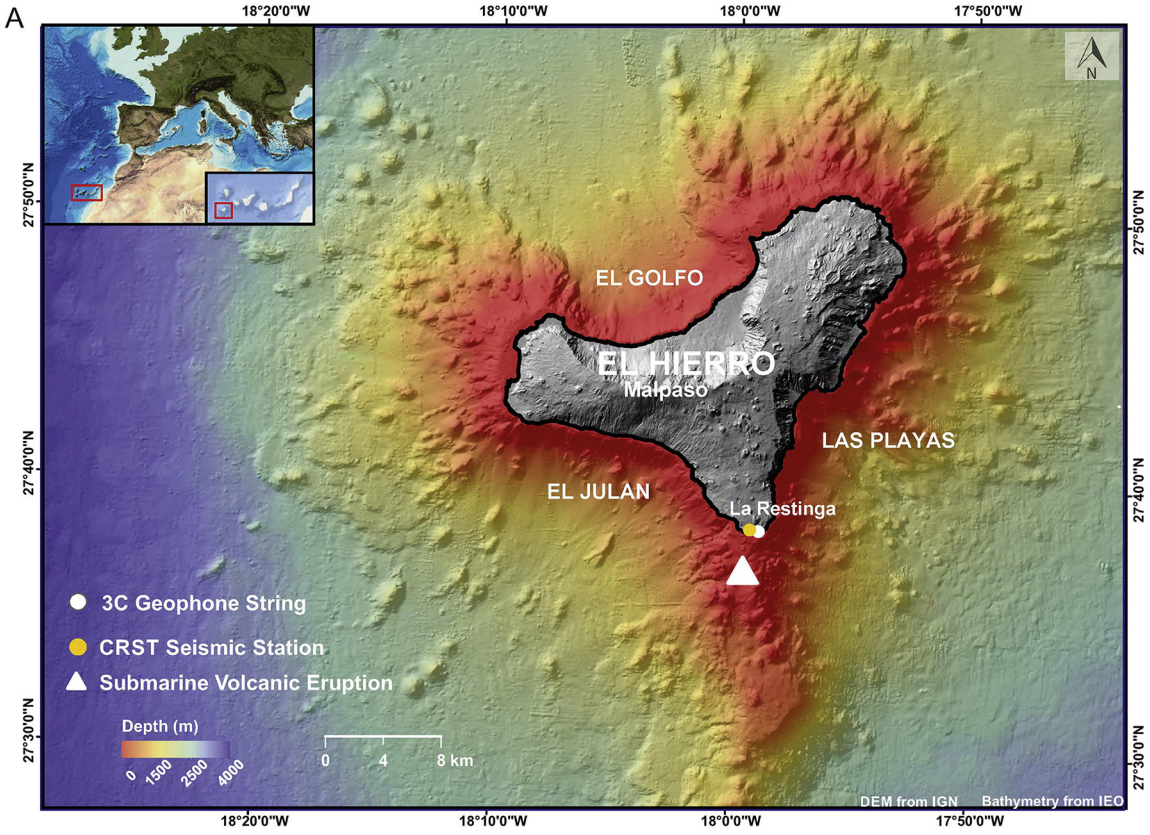

Fig. 1. A) Map of El Hierro Island showing topography and bathymetry; location of the 3C Geophone string array (white circle); the IGN 3C CRST seismic station (orange circle); and submarine volcanic eruption (white triangle). Inset: El Hierro Island and the location of the Canary Islands Archipelago, off the NW coast of Africa. B) La Restinga village with the location of the Geophone string array and the IGN seismic station. C) Geophone array final deployment.

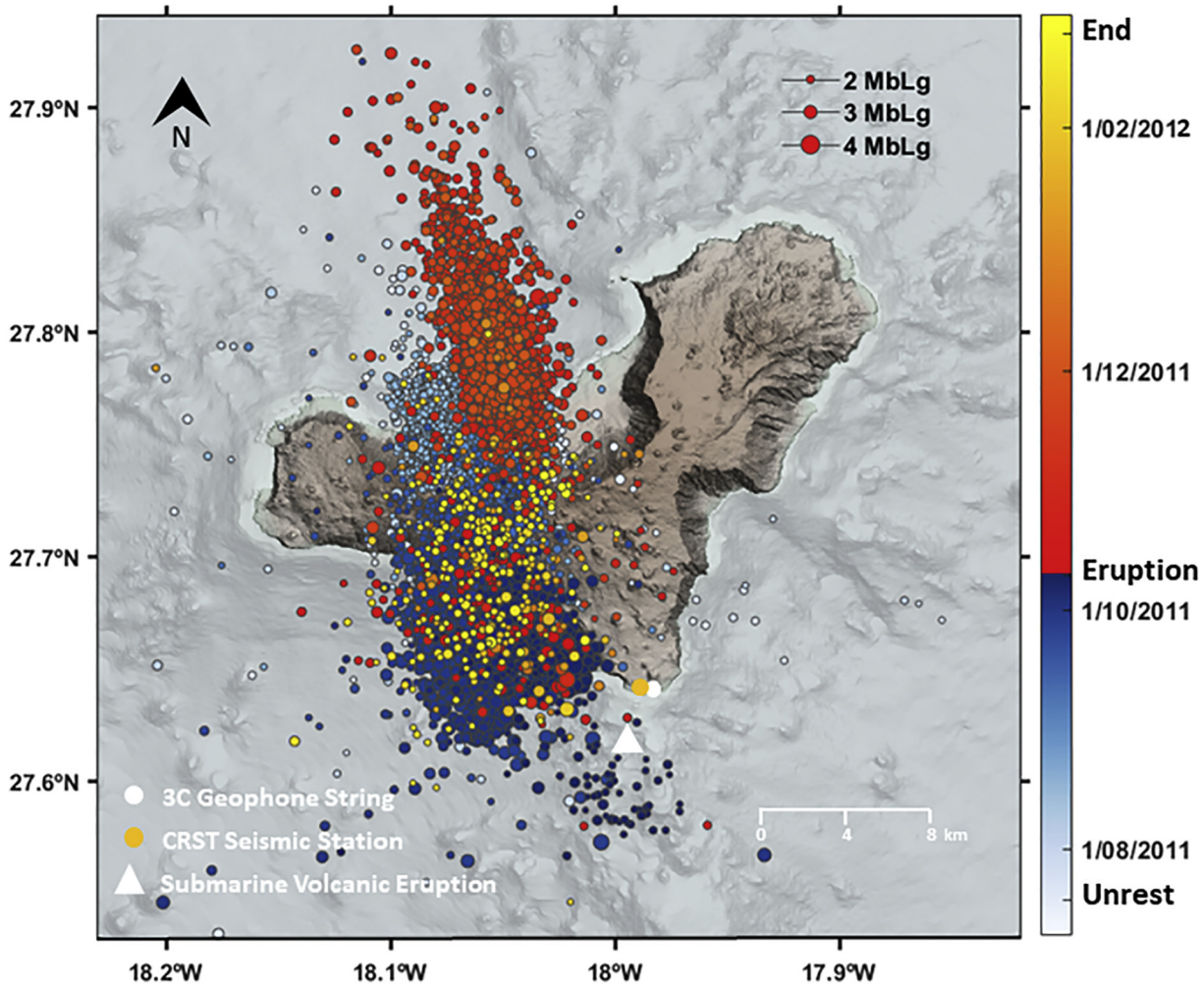

Fig. 2. Epicentral location of the seismic events recorded from July 19th, 2011 (beginning of the unrest phase) to October 10th, 2011 (date the eruption started) and from the beginning of the volcanic eruption on October 10th to February 27th, 2012 (end of the eruptive phase). Location of the 3C Geophone string array (white circle), the IGN 3C CRST seismic station (orange circle) and the submarine volcanic eruption (white triangle) are shown. Data from the IGN Seismic Catalogue (www.ign.es).

than 200 years of quiescence, a submarine volcanic eruption started on October 10th, 2011, less than 2 km off the island's southern coast (Fig. 1). El Hierro was the first ever instrumentally monitored eruption in the Canary Islands. It was also the first submarine eruption ever recorded in the Canary Islands. Three months before the beginning of the eruption, almost 10,000 earthquakes had been recorded, located at depths of 10–15 km (Fig. 2), ground deformation reached more than 5 cm, and gas emission anomalies were detected (López et al., 2012). From the beginning of the eruption, a continuous volcanic tremor was registered at all the seismic stations. During the first days of the eruption, the tremor signal dominated the associated weak seismicity. But by the end of October 2011 and for about five weeks thereafter, strong tectonic and volcano-tectonic seismicity was recorded, mostly concentrated at the north of the island, at a depth of about 25 km, and later, at just 10–15 km (Fig. 2). (López et al., 2012).

The eruption started at a sea floor water depth of 363 m (Rivera et al., 2013). Successive bathymetric surveys located the volcano summit at decreasing water depths: from 220 m to the last measured water depth of the volcano summit at 89 m (Rivera et al., 2013). The lavas mostly flowed from the volcano southwestwards towards the open ocean.

"Restingolites" were the first volcanic products that were observed and sampled, both floating on the sea surface and along the shores and beaches of El Hierro Island. These volcanic products were emitted during the first days of the eruption (October 15th to 17th) and have been petrologically described by different authors (Troll et al., 2012; Meletlidis et al., 2012; Sigmarsson et al., 2013; Del Moro et al., 2015) as consisting of an outer basanite crust embedding pumiceous xenoliths. The rest of the samples appeared a few days later, all basaltic without any contamination by silicic material in the form of floating lava balloons. From the beginning, a number of relevant sea-surface phenomena (lava fragments, stains, and bubbles) associated with the development of the eruption were observed in the area around the eruption site (Fig. S1). Throughout the eruption, La Restinga Harbor remained closed and the entire fleet was stranded. The inspection and reconnaissance work of the eruption area was carried out by oceanographic vessels and by the "Salvamar Adahara" vessel from the Canary Government.

4. Methods

In this study, we present the preliminary results obtained from the analysis of the continuous monitoring signals of the volcanic eruption at El Hierro in the Canary Islands using an underwater geophone array. We show its successful application and capacity to characterize events during submarine eruptions, demonstrating that it is also suitable for locating the source of submarine acoustic emissions.

In the same way as subaerial infrasonic arrays, an underwater geophone array can discriminate the acoustic waves that are generated by a source and therefore allow it to be localized and characterized. It is

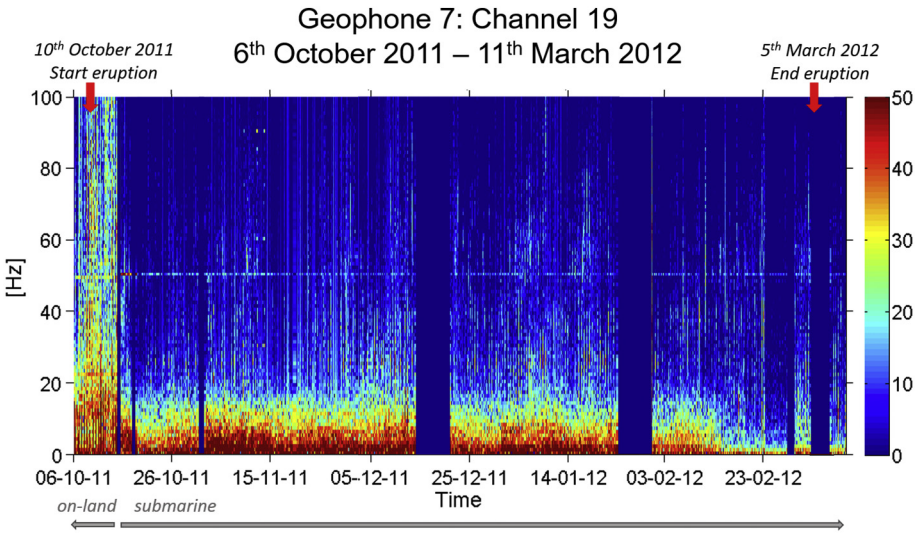

Fig. 3. Instrument corrected spectrogram of the available data recorded from October 2011 to March 2012, by the 19th channel (vertical component) of the geophone array. Represented a subset of the data total range. From 06th October to 16th October 2011, the array was installed on-land, in the Volcano Observatory Office in Valverde (El Hierro), 25 km away from La Restinga.

well known that the formation of bubbles and the expulsion of steam and volcanic material produces a significant underwater sound (Ichihara et al., 2009; Chadwick et al., 2008a). Given that El Hierro eruption was submarine, the recording of the eruption acoustic signals presented a challenge.

4.1. The acoustic array in La Restinga Harbor: A new approach to volcanic activity signal acquisition and volcanic activity monitoring

During a volcanic eruption, the sudden ejection of material occurs and a broad spectrum of pressure oscillations is generated—from infrasonic to gravity waves (e.g., Johnson and Ripepe, 2011; Fee and Matoza, 2013). Therefore, arrays of acoustic sensors, deployed as small antennas or distributed at various azimuths around the volcano, represent a unique opportunity for enhanced event detection and localization (Ripepe and Marchetti, 2002; Garcés et al., 2008; Yamakawa et al., 2018).

Acoustic pressure is largely used to monitor volcanic activity and has become one of the most promising techniques to calculate magma overpressure and flux of a volcanic eruption. The relationship between acoustic pressures and flux vary depending on the model assumed (Ichihara, 2016). This can be also monitored remotely (Caplan-Auerbach et al., 2010; Johnson and Ripepe, 2011; Kim et al., 2015; Fee and Matoza, 2013). Submarine volcanic eruptions have only been directly monitored for two cases (Resing et al., 2011; Chadwick et al., 2008b) and no standardized procedure or methodology exists at present. To this end, we have designed an innovative approach using an array of underwater geophones. The array was installed for the purpose of recording and monitoring submarine volcanic activity.

4.2. Acquisition with the submarine acoustic array in La Restinga Harbor

From the beginning of the eruption in October 2011, IGN-CSIC deployed an array of eight, 3-component, 6 m spacing cable-connected geophones in La Restinga Harbor (Fig. S2), recording data continuously. Each geophone consists on a Geospace Omni-2400 module based on three orthogonal independent sensors that measure ground velocity. The 24 channels were sampled at 250 Hz. The instrument response of the geophones and the IGN 3C CRST broadband seismic stations are shown in Fig. S3. This experimental setting allowed us to successfully record sample data from October 16th, 2011 to May 2nd, 2012. The geophone array was deployed less than 2 km from the submarine volcanic vent and near the southern coast of the island, close to La Restinga village on the harbor's sea floor, at a variable depth ranging between 6 and 12 m below sea level (Fig. S4). The array was placed by divers directly on the sea floor some of the sensors being partially buried in the sandy bottom. Due to the physical characteristics of the sensors, and the difficult conditions of the place where the geophones were positioned, it was not possible to orient the three components of the geophones at the time of the initial installation. Once the eruption ended, and before retrieving the geophones, a test was conducted to establish the orientation of the horizontal component of the geophones. This test was carried out by a professional diver, who applied the taps by slightly touching the geophones with his finger. An X-Y graph was generated for each tap, using the horizontal (Channel X) and vertical components (Channel Y) of the geophones, and then plotting the horizontal and vertical data in an X-Y plot. Linear fitting of the data allowed estimating the angle of rotation.

The data were transmitted by cable in real time to an acquisition station on the surface, digitized with a Geode (Geometrics) 24-channel seismometer, and stored on a laptop computer. As the acquisition system was not designed for a long-term continuous acquisition; a frequent maintenance was needed in order to solve power problems, yet it was possible to maintain more than 90% data availability. In Fig. 3 we show the entire spectrogram of the available data recorded from October 2011 to March 2012. The geophone spectrogram was computed by using a 50% overlapping (10-min) sliding window, and applying spectra correction using the instrument response.

4.3. Comparing seismic and acoustic signals

In order to compare seismic and acoustic signals, we selected periods with relevant eruptive activity. In Fig. 4 we compare the seismic signal and the spectrogram, acquired by the CRST seismic station of IGN, to the acoustic signal recorded by the 19th channel of geophone number 7 of the geophone array. A good correspondence between the two signals can be observed.

The geophone and seismic spectrograms were computed by using a 50% overlapping 30-s sliding window, applying a spectra correction using instrument response. The two raw data signals are in general quite similar, indicating that in spite of the differences between the two instruments, they are recording the same events—especially during

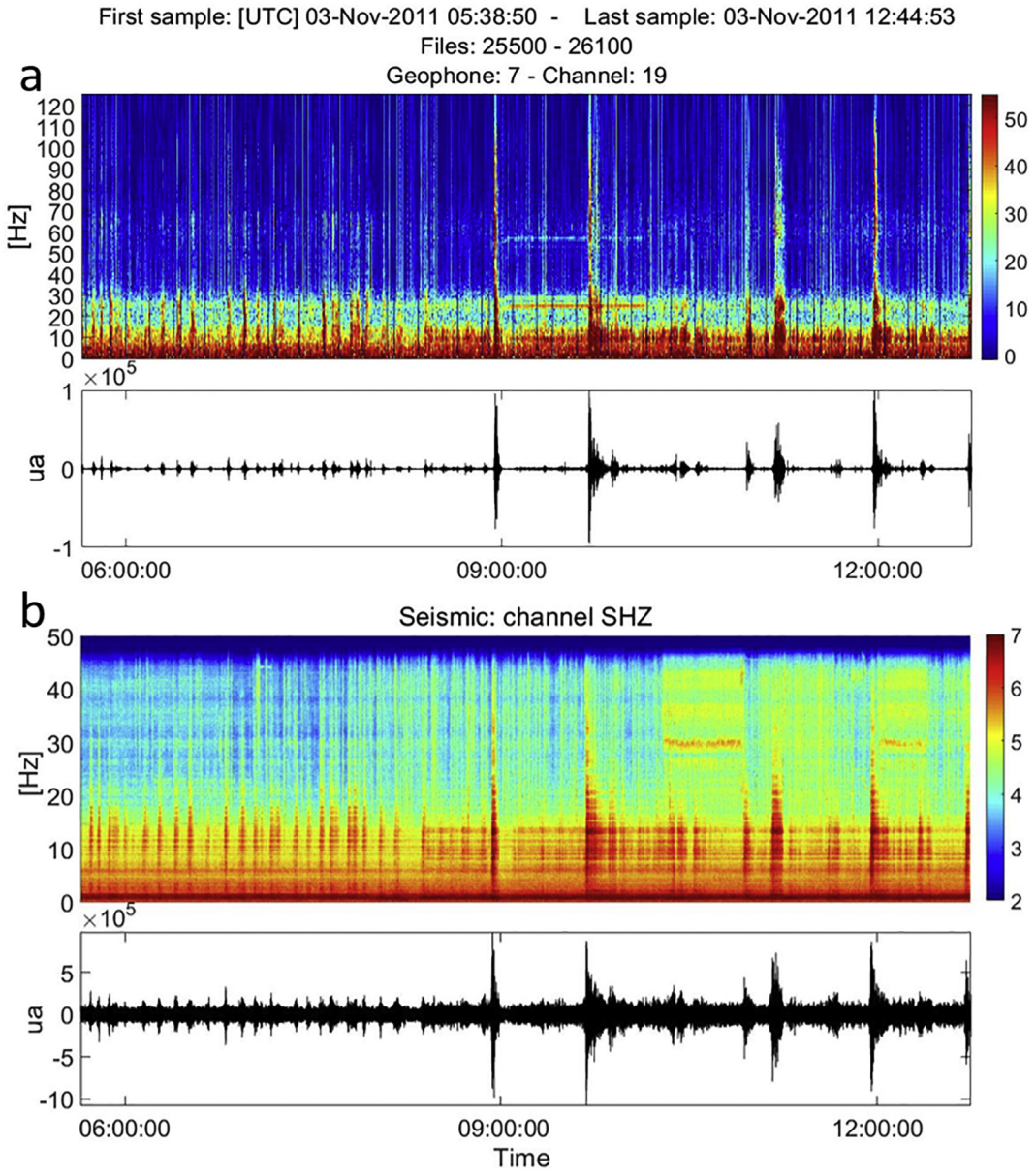

Fig. 4. Comparison of spectrogram and seismic signal for a recording interval of more than 6 h: a) seismic signal recorded by CRST station, and b) acoustic signals recorded by one of the channels of the geophone array on November 3rd, 2011.

intense seismicity. They show differences in spectra, due to the higher sampling rate of the geophone array. The seismic station with 100 Hz sampling provides information lower than 50 Hz, while the geophone array due to the 250 Hz sampling can reach 125 Hz (Fig. 4). During the phases of intense degasification, and also during phases of ash and rock sample emission, both the time and spectral signals show important differences. This indicates that the geophone array is capable of recording information transmitted not only by the seafloor but also traveling through the water. As an example, we display in Fig. 5 both the spectrograms and raw data of the geophone array and the seismic land station CRST, recorded in 2011 (October 16–17th) and 2012 (February 4–5th) respectively. The signal labeled A and C on the Fig. 5 geophone spectrograms could be related to observed surface events associated with the eruption. The signal labeled B could be caused by the sonar signal used in the eruption area during inspection activities, given that during the time the eruption was active, all other marine activity (diving, fishing, sailing) were banned. The energetic events A, B, C detected by the geophone were not registered by the seismic station on land. The high frequency signal (C) recorded by the geophone array coincides with the observation on the sea surface of intense gas and ash emission activity. The interpretation of signal labeled B, recorded in all the geophone channels, remains unclear.

4.4. Locating an underwater source

One of the main goals of this study was to locate the underwater source during the eruption. In order to locate the acoustic signal source, we calculated the wave field energy distribution around the array. The methodology we applied for the location of the source is based on two basic assumptions: i) the source is isotropic and ii) seismic polarization at wavelengths larger than the source-receiver distance is representative of the source position.

We assumed the source is the point where a spherical wave field accommodates the maximum energy at the array. Then, assuming a back azimuth, θ and takeoff angle, i, the acoustic amplitude, u at each geophone of the string can be expressed as:

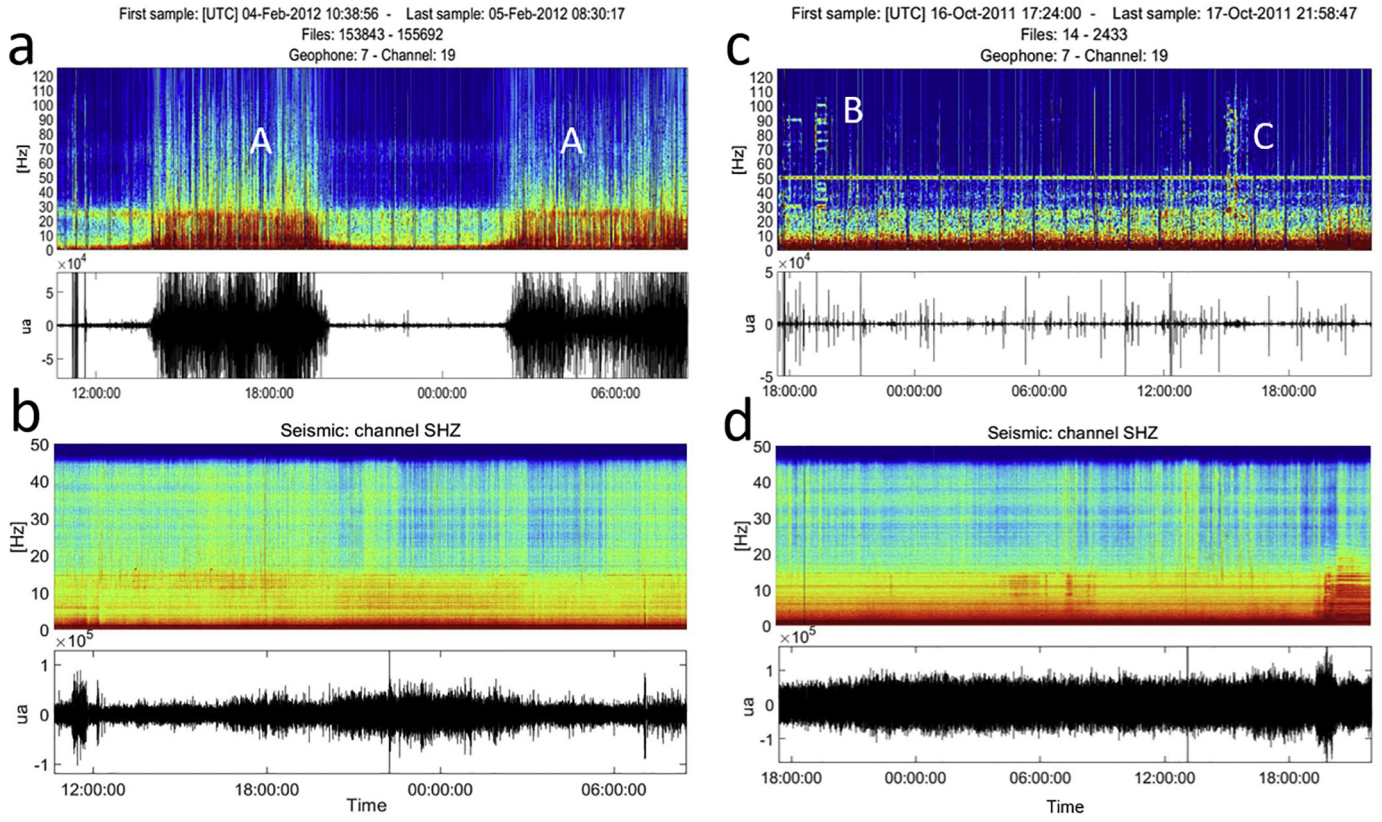

Fig. 5. Spectrograms and raw data of the underwater geophone array (quadrants a, c) and the seismic land station CRST (quadrants b, d), recorded on February 4–5th, 2012 and October 16–17th, 2011. Signals labeled A, B, and C points to the events detected by the geophone that were not registered by the seismic station on land.

$$u(t,\theta,i) = [u_1(t)cos\theta + u_2(t)sin\theta]\ sin\ i + u_3(t)\ cosi \quad (1)$$

where *u1*, *u2*, and *u3* are the acoustic vector components in the N-S, E-W, and vertical directions, respectively. From the vector $u(t,\theta,i)$, the acoustic energy around the array can be calculated as:

$$E(\theta,i) = \frac{1}{\tau}\int_t^{t+\tau} u^2(t,\theta,i)dt \quad (2)$$

where the direction of the propagating wavefront (Fig. 6) is given by the back azimuth with the maximum energy $E(\theta,i)$. However, the energy distribution is twofold and it has two maxima in opposite directions: θ and $\theta + 180°$, reflecting the polarity of the acoustic wave (Fig. 6). To solve this ambiguity, we calculated the theoretical arrival times for each back azimuth θ and $\theta + 180°$. We then time-shifted the vertical components of each geophone and calculated the multicomponent semblance to define the true back azimuth among the two possible directions. This assumes that the waves are propagating from the $(\theta, \theta + 180°)$ direction and that the velocities of the acoustic waves propagate along the geophone string array direction.

5. Results

The submarine acoustic array deployed off the coast of El Hierro presents for the first time, a unique example of remote submarine monitoring of volcanic activity. Our results show that acoustic waves were recorded by the array deployed inside the waters of La Restinga (El Hierro) Harbor, which was confirmed by the strong correlation to the seismic waves recorded by the seismic station and network on land.

The spectral content is different for the two wave fields recorded by the submarine array and seismic station (Figs. 4, 5) showing how the same source is partitioning the energy differently in the ground and in the water. Our analysis indicates consistency between infrasound and seismic waves generated by subaerial volcanic activity (Fig. 5). This observation suggests close coupling of the source with the ground and the water and thus, efficient propagation of the signal at the ground-water interface. Even though the geometry of the linear string of geophones is not the best for the proper location of the source, we could define the distribution of the energy propagation with two back azimuths (Fig. 6) ranging between $30 \pm 5°$N, (θ), and $210 \pm 5°$N $(\theta + 180°)$. However, we indeed found evidence to support the assumption that the wave

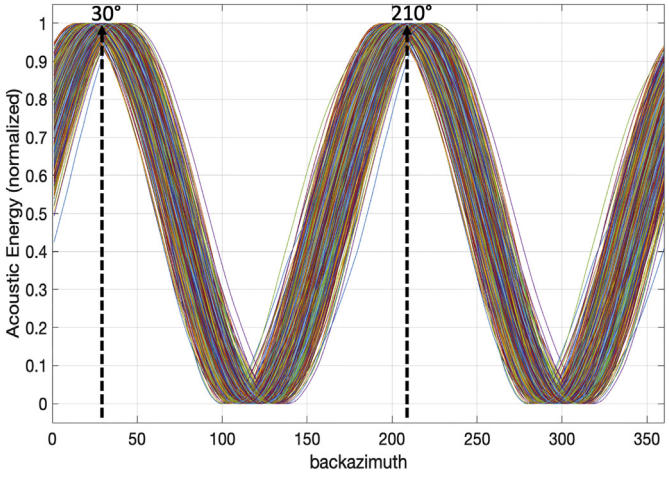

Fig. 6. One day (29/01/2012) of energy distribution (Eq. 2) around the string calculated for a 4 s long time window shifted by 1 s. The analysis indicates that acoustic energy in the frequency band 1–20 Hz reaches the maximum values for two different backazimiuths (θ) at ~30° and ~210° North.

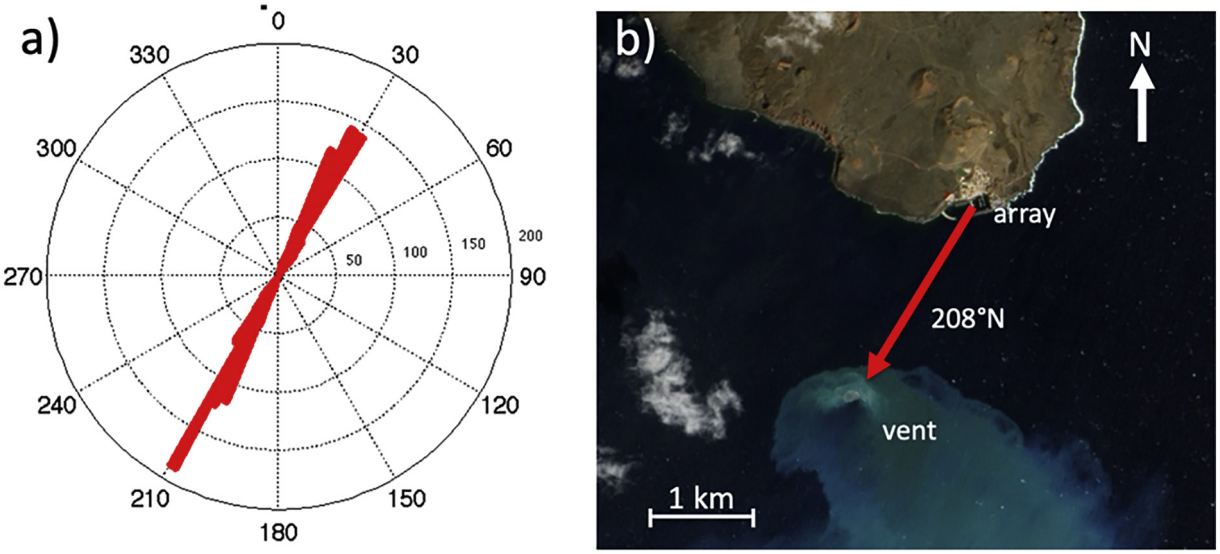

Fig. 7. a) Back azimuth (θ) calculated (Eq. 2) for three days (3/11/2011, 7/11/2011, and 29/01/2012) in consecutive time windows 4 s long shifted by 1 s; it is very stable and ranges between 205 and 215°N. b) The most recurrent back-azimuth, indicated with the red arrow, points to 208°N towards the position of the eruptive vent. (Source: NASA Earth Observatory image using EO-1 ALI data).

field recorded by the geophones was propagating inside the water column.

The higher semblance values of >0.8 for back azimuths range from 205 to 215°N, indicating a propagation velocity of 1510 m/s. This acoustic velocity is slightly higher but still consistent with the average velocity of sound in shallow water (c = 1484 m/s), meaning that the maximum energy corresponds to the arrival of acoustic waves propagating from the eruption site to the geophone string through the water. We cannot eliminate the possibility that seismic waves recorded by the geophone string had propagated also through the seafloor rocks. The back-azimuth direction of wave propagation is compatible with the position of the submarine volcano's eruptive vent and it coincides with the surface manifestations of the sea surface volcanic activity in the area (Fig. 7).

Our results show that the data recorded with the underwater geophone array is adequate for the detection of the high-frequency content of the eruptive activity, but also to locate its source and to show that it is sensitive enough for recording other events that were not recorded by the onshore seismic stations.

6. Discussion and conclusions

Only recently, the development of new technology has shown that monitoring submarine volcanoes is technically feasible but that characterization and understanding of submarine volcanism remains incipient when compared to the characterization of subaerial volcanism.

In the last years, the results obtained by hydroacoustic arrays, mostly installed in the Pacific Ocean (Caplan-Auerbach and Duennebier, 2001; Chadwick et al., 2008a, 2008b) have been very promising towards the goal of monitoring submarine volcanic activity, and today represent a remarkable new tool to characterize these events.

Our results were obtained by combining land and submarine continuous seismic monitoring of a submarine volcanic eruption for the first time. The submarine monitoring was performed by using a geophone array deployed on the seabed off the coast of El Hierro, Canary Islands, Spain.

With this original monitoring, the dataset and results obtained cover most of the syn-eruptive activity as well as different eruptive phases, from the beginning of the eruption to the last phases of eruptive activity.

Our results show consistency with well-documented subaerial activity (gas and ash emission, lava balloon emissions, and other processes) as well as with the data and results obtained from seismic network data (seismic catalogue).

One of the most valuable results is the high accuracy for determining the azimuth of the acoustic source by applying array techniques on the data recorded with a geophone array. Moreover, these results are consistent with the known location of the submarine volcanic eruption.

Acoustic waves traveled at 1510 m/s, compatible with the speed of sound in the water. Therefore, wave propagation was performed likely through the water, not being able to discard partial body wave propagation through the ocean crust, near the seafloor.

Our results and experience obtained from monitoring the El Hierro eruption with complementary techniques supports the idea that acoustic arrays can be successfully used at sea just as infrasonic arrays are successfully used on land to locate the source of acoustic emissions underwater. As presented in the introduction previous studies have demonstrated that acoustic arrays can locate the source of acoustic emissions underwater. Therefore, acoustic arrays should be regarded as a valuable tool for hazard and risk assessments for populations living in the coastal areas.

In our study we demonstrate the ability of small aperture acoustic arrays to identify underwater gravitational instability phenomena, even at considerable distances (and not necessarily related to eruptive activity) makes them undoubtedly useful as a complementary tool for the implementation of tsunami rapid alert systems.

Our results show the utility of introducing this type of new and innovative methodology for long-term submarine volcanic activity monitoring and characterization.

Availability of data and material

The data analyzed in this study is a subset of a complete dataset recorded during the eruption. Once ongoing research on this dataset is finalized, CSIC data will be available through the Digital.CSIC data repository.

Funding

M.J. Jurado's research was funded by the Spanish Ministry project CGL2010-21568.

Authors' contributions

M.J. Jurado, C. Lopez, M.J. Blanco designed, implemented and maintained the experimental monitoring system and supervised the data quality and performance of the geophone array and seismograph during the submarine eruption. They also established correlations of events observed on the sea surface and some events characterized on the seismic network database and the data acquired in La Restinga hydroacoustic monitoring station. Furthermore, they processed the data and analyzed in the detail the correlation of events recorded by the IGN seismic network. Maurizio Ripepe, Antonio Ricciardi, and Giorgio Lacanna carried out the analysis of the data and addressed the characterization and azimuth of the tremor source by applying array techniques on the data recorded with the hydroacoustic array. All the results were discussed by all the authors and reported in this manuscript. The manuscript was iteratively revised by the co-authors.

Declaration of Competing Interest

None.

Acknowledgments

M.J. Jurado's research was funded by the Spanish Ministry project CGL2010-21568. We would like to thank wholeheartedly our colleagues and friends from the IGN, Civil Protection, Pinar Council, and Canary Islands Government, and the volunteer divers. Also Inma and Francisco from La Restinga (Bar La Laja), who helped supervising the continuous operation of the instrumentation during the volcanic eruption. All of them helped to make possible the acquisition of the observational data used in this study. We also would like to thank Salvamar Adhara's crew for their cooperation in observing the submarine eruption and for samples collection at sea. Rafael Abella for his contribution to processing methodology. We thank also Sergio Capuz for his assistance in data processing. The English text was reviewed and revised by Grant George Buffett (www.terranova.barcelona). Two anonymous reviewers for their revision and inputs to improve the paper.

Appendix A. Supplementary data

Supplementary data to this article can be found online at https://doi.org/10.1016/j.jvolgeores.2020.107097.

References

Becerril, L., Cappello, A., Galindo, I., Neri, M., Del Negro, C., 2013. Spatial probability distribution of future volcanic eruptions at El Hierro Island (Canary Islands, Spain). J. Volcanol. Geotherm. Res. 257, 21–30.

Caplan-Auerbach, J., Bellesiles, A., Fernandes, J.K., 2010. Estimates of eruption velocity and plume height from infrasonic recordings of the 2006 eruption of augustine volcano, alaska. J. Volcanol. Geotherm. Res. 189, 12–18.

Caplan-Auerbach, J., Dziak, R.P., Bohnenstiehl, D.R., Chadwick, W.W., Lau, T.K., 2014. Hydroacoustic investigation of submarine landslides at West Mata volcano, Lau Basin. Geophys. Res. Lett. 41 (16), 5927–5934.

Caplan-Auerbach, J., Dziak, R.P., Haxel, J., Bohnenstiehl, D.R., Garcia, C., 2017. Explosive processes during the 2015 eruption of Axial Seamount, as recorded by seafloor hydrophones. Geochem. Geophys. Geosyst. 18 (4), 1761–1774.

Carracedo, J.C., 1994. The Canary Islands: an example of structural control on the growth of large oceanic-island volcanoes. J. Volcanol. Geotherm. Res. 60 (3–4), 225–241.

Chadwick, W.W., Wright, I.C., Schwarz-Schampera, U., Hyvernaud, O., Reymond, D., De Ronde, C.E., 2008a. Cyclic eruptions and sector collapses at Monowai submarine volcano, Kermadec arc: 1998–2007. Geochem. Geophys. Geosyst. 9 (10).

Chadwick, W.W., Cashman, K.V., Embley, R.W., Matsumoto, H., Dziak, R.P., De Ronde, C.E., Lau, T.K., Deardorff, N.D., Merle, S.G., 2008b. Direct video and hydrophone observations of submarine explosive eruptions at NW Rota-1 volcano, Mariana arc. J. Geophys. Res. Solid Earth 113 (B8).

Chadwick, W.W., Dziak, R.P., Haxel, J.H., Embley, R.W., Matsumoto, H., 2012. Submarine landslide triggered by volcanic eruption recorded by in situ hydrophone. Geology 40, 51–54.

Del Moro, S., Di Roberto, A., Meletlidis, S., Pompilio, M., Bertagnini, A., Agostini, S., Ridolfi, F., Renzulli, A., 2015. Xenopumice erupted on 15 October 2011 offshore of El Hierro (Canary Islands): a subvolcanic snapshot of magmatic, hydrothermal and pyrometamorphic processes. Bull. Volcanol. 77 (6), 53.

Dziak, R.P., Haxel, J.H., Matsumoto, H., Lau, T.K., Merle, S.G., De Ronde, C.E., Embley, R.W., Mellinger, D.K., 2008. Observations of regional seismicity and local harmonic tremor at Brothers volcano, south Kermadec arc, using an ocean bottom hydrophone array. J. Geophys. Res. Solid Earth 113 (B8).

Dziak, R.P., Bohnenstiehl, D.R., Baker, E.T., Matsumoto, H., Caplan-Auerbach, J., Embley, R. W., Chadwick Jr., W.W., 2015. Long-term explosive degassing and debris flow activity at West Mata submarine volcano. Geophys. Res. Lett. 42 (5), 1480–1487.

Fee, D., Matoza, R.S., 2013. An overview of volcano infrasound: from Hawaiian to Plinian, local to global. J. Volcanol. Geotherm. Res. 249, 123–139.

Forjaz, V.H., 2000. Vulcão Oceânico da Serreta. Observatório Vulcanológico e Geotérmico dos Açores, Ponta Delgada.

Fox, C.G., Matsumoto, H., Lau, T.K., 2001. Monitoring Pacific Ocean seismicity from an autonomous hydrophone array. J. Geophys. Res. Solid Earth 106 (B3), 4183–4206.

Garcés, M., Fee, D., Steffke, A., McCormack, D., Servranckx, R., Bass, H., Hetzer, C., Hedlin, M., Matoza, R., Yepes, H., Ramon, P., 2008. Capturing the acoustic fingerprint of stratospheric ash injection. EOS Trans. Am. Geophys. Union 89 (40), 377–378.

Guillou, H., Carracedo, J.C., Torrado, F.P., Badiola, E.R., 1996. K-Ar ages and magnetic stratigraphy of a hotspot-induced, fast grown oceanic island: El Hierro, Canary Islands. J. Volcanol. Geotherm. Res. 73 (1–2), 141–155.

Hernández, P.A., Calvari, S., Ramos, A., Pérez, N.M., Márquez, A., Quevedo, R., Barrancos, J., Padrón, E., Padilla, G.D., López, D., Santana, Á.R., 2014. Magma emission rates from shallow submarine eruptions using airborne thermal imaging. Remote Sens. Environ. 154, 219–225.

Ichihara, M., 2016. Seismic and infrasonic eruption tremors and their relation to magma discharge rate: A case study for sub-Plinian events in the 2011 eruption of Shinmoe-dake, Japan. J. Geophys. Res. Solid Earth 121, 7101–7118. https://doi.org/10.1002/2016JB013246.

Ichihara, M., Ripepe, M., Goto, A., Oshima, H., Aoyama, H., Iguchi, M., Tanaka, K., Taniguchi, H., 2009. Airwaves generated by an underwater explosion: Implications for volcanic infrasound. J. Geophys. Res. 114, B03210. https://doi.org/10.1029/2008JB005792.

Johnson, J.B., Ripepe, M., 2011. Volcano infrasound: a review. J. Volcanol. Geotherm. Res. 206 (3–4), 61–69.

Kaneko, Takayuki, Maeno, Fukashi, Yasuda, Atsushi, Takeo, Minoru, Takasaki, Kenji, 2019. The 2017 Nishinoshima eruption: combined analysis using Himawari-8 and multiple high-resolution satellite images. Earth Planets Space 71. https://doi.org/10.1186/s40623-019-1121-8.

Kim, K., Fee, D., Yokoo, A., Lees, J.M., 2015. Acoustic source inversion to estimate volume flux from volcanic explosions. Geophys. Res. Lett. 42, 5243–5249.

Kokelaar, B.P., Durant, G.P., 1983. The submarine eruption and erosion of Surtla (Surtsey), Iceland. J. Volcanol. Geotherm. Res. 19 (3–4), 239–246.

López, C., Blanco, M.J., Abella, R., Brenes, B., Cabrera-Rodríguez, V.M., Casas, B., Domínguez-Cerdeña, I., Felpeto, A., Fernández de Villalta, M., del Fresno, C., García-Arias, M.J., García-Cañada, L., Gomis-Moreno, A., González-Alonso, E., Guzmán-Pérez, J., Iribarren, I., López-Díaz, R., Luengo-Oroz, N., Meletlidis, S., Moreno, M., Moure, D., Pereda de Pablo, J., Rodero, C., Romero, E., Sainz-Maza, S., Sentre-Domingo, M.A., Torres, P.A., Trigo, P., Villasante-Marcos, V., 2012. Monitoring the volcanic unrest of El Hierro (Canary Islands) before the onset of the 2011-2012 submarine eruption. Geophys. Res. Lett. 39, LI3303. https://doi.org/10.1029/2012GL051846.

Lyons, J.J., Haney, M.M., Fee, D., et al., 2019. Infrasound from giant bubbles during explosive submarine eruptions. Nat. Geosci. 12, 952–958. https://doi.org/10.1038/s41561-019-0461-0.

Lyons, J.J., Iezzi, A., Fee, D., et al., 2020. Infrasound generated by the 2016–2017 shallow submarine eruption of Bogoslof volcano, Alaska. Bull. Volcanol. 82, 19. https://doi.org/10.1007/s00445-019-1355-0.

Meletlidis, S., Di Roberto, A., Pompilio, M., Bertagnini, A., Iribarren, I., Felpeto, A., Torres, P. A., D'Oriano, C., 2012. Xenopumices from the 2011–2012 submarine eruption of El Hierro (Canary Islands, Spain): constraints on the plumbing system and magma ascent. Geophys. Res. Lett. 39 (17).

Nishida, K., Ichihara, M., 2016. Real-time infrasonic monitoring of the eruption at a remote island volcano using seismoacoustic cross correlation. Geophys. J. Int. 204 (2), 748–752.

Ripepe, M., Marchetti, E., 2002. Array tracking of infrasonic sources at Stromboli Volcano. Geophys. Res. Lett. 29 (22).

Rivera, J., Lastras, G., Canals, M., Acosta, J., Arrese, B., Hermida, N., Micallef, A., Tello, O., Amblas, D., 2013. Construction of an oceanic island: Insights from the El Hierro (Canary Islands) 2011–2012 submarine volcanic eruption. Geology. 41 (3), 355–358.

Schnur, S.R., Chadwick Jr., W.W., Embley, R.W., Ferrini, V.L., de Ronde, C.E., Cashman, K.V., ... Matsumoto, H., 2017. A decade of volcanic construction and destruction at the summit of NW Rota-1 seamount: 2004–2014. J. Geophys. Res. Solid Earth 122 (3), 1558–1584.

Shinohara, M., Ichihara, M., Sakai, S., et al., 2017. Continuous seismic monitoring of Nishinoshima volcano, Izu-Ogasawara, by using long-term ocean bottom seismometers. Earth Planets Space 69, 159 https://doi.org/10.1186/s40623-017-0747-7.

Sigmarsson, O., Laporte, D., Carpentier, M., Devouard, B., Devidal, J.L., Marti, J., 2013. Formation of U-depleted rhyolite from a basanite at El Hierro, Canary Islands. Contrib. Mineral. Petrol. 165 (3), 601–622.

Sugioka, H., Fukao, Y., Hibiya, T., 2005. Submarine volcanic activity, ocean-acoustic waves and internal ocean tides. Geophys. Res. Lett. 32 (24). https://doi.org/10.1029/2005GL024001.

Tepp, G., Chadwick, W.W., Haney, M.M., Lyons, J.J., Dziak, R.P., Merle, S.G., et al., 2019. Hydroacoustic, seismic, and bathymetric observations of the 2014 submarine eruption at Ahyi Seamount, Mariana Arc. Geochem. Geophys. Geosyst. 20, 3608–3627. https://doi.org/10.1029/2019GC008311.

Thorarinsson, S., Einarsson, T., Sigvaldason, G., Elisson, G., 1964. The submarine eruption off the Vestmann Islands 1963–64. Bull. Volcanol. 27 (1), 435–445.
Troll, V.R., Klugel, A., Longpré, M.A., Burchardt, S., Deegan, F.M., Carracedo, J.C., Wiesmaier, S., Kueppers, U., Dahern, B., Hansteen, T.H., Freda, C., 2012. Floating stones off El Hierro, Canary Islands: xenoliths of pre-island sedimentary origin in the early products of the October 2011 eruption. Solid Earth 3, 97–110.
Villasante-Marcos, V., Pavón-Carrasco, F.J., 2014. Paleomagnetic constraints on the age of Lomo Negro volcanic eruption (El Hierro, Canary Islands). Geophys. J. Int. 199, 1497–1514. https://doi.org/10.1093/gji/ggu346.
Wilcock, W.S.D., Tolstoy, M., Waldhauser, F., Garcia, C., Tan, Y.J., Bohnenstiehl, D.R., Caplan-Auerbach, J., Dziak, R.P., Arnulf, A., Mann, M.E., 2016. Seismic constraints on caldera dynamics from the 2015 Axial Seamount eruption. Science 354, 1395–1399.
Yamakawa, K., Ichihara, M., Ishii, K., Aoyama, H., Nishimura, T., Ripepe, M., 2018. Azimuth estimations from a small aperture infrasonic array: Test observations at Stromboli volcano, Italy. Geophys. Res. Lett. 45, 8931–8938 https://doi.org/10.1029/2018GL078851.